ORIGINAL PAPER

Supratentorial and spinal pediatric ependymomas display a hypermethylated phenotype which includes the loss of tumor suppressor genes involved in the control of cell growth and death

**Hazel A. Rogers · John-Paul Kilday · Cerys Mayne · Jennifer Ward ·
Martyna Adamowicz-Brice · Ed C. Schwalbe · Steven C. Clifford ·
Beth Coyle · Richard G. Grundy**

Abstract Epigenetic alterations, including methylation, have been shown to be an important mechanism of gene silencing in cancer. Ependymoma has been well characterized at the DNA copy number and mRNA expression levels. However little is known about DNA methylation changes. To gain a more global view of the methylation profile of ependymoma we conducted an array-based analysis. Our data demonstrated tumors to segregate according to their location in the CNS, which was associated with a difference in the global level of methylation. Supratentorial and spinal tumors displayed significantly more hypermethylated genes than posterior fossa tumors, similar to the 'CpG island methylator phenotype' (CIMP) identified in glioma and colon carcinoma. This hypermethylated profile was associated with an increase in expression of genes encoding for proteins involved in methylating DNA, suggesting an underlying mechanism. An integrated analysis of methylation and mRNA expression array data allowed us to identify methylation-induced expression changes. Most notably genes involved in the control of cell growth and death and the immune system were identified, including members of the JNK pathway and PPARG. In conclusion, we have generated a global view of the methylation profile of ependymoma. The data suggests epigenetic silencing of tumor suppressor genes is an important mechanism in the pathogenesis of supratentorial and spinal, but not posterior fossa ependymomas. Hypermethylation correlated with a decrease in expression of a number of tumor suppressor genes and pathways that could be playing an important role in tumor pathogenesis.

Keywords Ependymoma · Methylation · JNK pathway · Apoptosis · Immune system

H. A. Rogers · J.-P. Kilday · C. Mayne · J. Ward ·
M. Adamowicz-Brice · B. Coyle · R. G. Grundy (✉)
Children's Brain Tumour Research Centre, D Floor Medical
School, Queen's Medical Centre, University of Nottingham,
Nottingham NG7 2UH, UK
e-mail: richard.grundy@nottingham.ac.uk

E. C. Schwalbe · S. C. Clifford
Northern Institute for Cancer Research, Newcastle University,
Newcastle upon Tyne, UK

Introduction

Ependymoma is the third most common pediatric tumor of the central nervous system (CNS), accounting for 6–12% of brain tumors in children. Prognosis for patients with ependymoma is relatively poor with a 5 year overall survival rate of 24–75% [68, 75]. Currently tumors are treated by surgical resection followed by radiotherapy, with the extent of resection one of the most consistent prognostic markers. Ependymomas are found intracranially and in the spinal cord. 90% of pediatric cases occur intracranially with 70% arising in the posterior fossa.

Molecular profiling has revealed genetic and transcriptional differences between tumors arising in different locations. Copy number analysis using CGH and array CGH [48, 62], and more recently, high resolution SNP arrays [28], has demonstrated location specific differences. Analysis of global transcriptional profiling data has also revealed distinct location based signatures, based on both mRNA and miRNA expression [28, 48, 52, 62]. Studies

suggest ependymomas from different locations arise from distinct populations of neural stem cells which may help explain the observed location based biological differences [28, 62]. Despite the large amount of molecular data generated, very few candidate genes and pathways have been identified in ependymoma that could be used in a more targeted approach to therapy [40].

Epigenetic changes, such as methylation, are frequently seen in a variety of tumors and provide an alternative mechanism from deletion or mutation for silencing of tumor suppressor genes. DNA methylation is mediated by DNA methyltransferase enzymes (DNMT1, DNMT3A, DNMT3B) which transfer a methyl group to cytosines found within CpG dinucleotides [5, 23]. This allows a complex containing methyl-CpG binding domain proteins to bind to the methylated DNA. The complex interacts with histone deacetylases, histone methyltransferases and chromatin remodeling enzymes to alter the chromatin into a state that is transcriptionally repressive [6].

To date only a few studies have analyzed methylation changes in ependymoma using a candidate gene approach. Tumor suppressor genes including CDKN2A, CDKN2B, HIC1, RASSF1A, CASP8, MGMT, and TP73 have been shown to be hypermethylated in ependymomas [2, 22, 46, 58, 64].

To gain a more global view of the methylation profile of ependymoma we utilized the GoldenGate Methylation Cancer Panel I (Illumina, San Diego, CA, USA). This array measures the methylation level of up to 1,505 independent CpG sites, representing 807 genes, which include known tumor suppressor genes and oncogenes, plus genes involved in cellular functions such as DNA repair, cell cycle control, differentiation and apoptosis. Our analysis of a cohort of 98 ependymomas revealed a difference in the global level of methylation between tumors arising in different locations. Tumors from a supratentorial or spinal location displayed a hypermethylated profile which was associated with an increased expression of genes encoding for proteins that form part of the DNA methylation machinery, suggesting an underlying mechanism. An integrated analysis of methylation and mRNA expression data allowed us to identify methylation-induced expression changes. Most notably genes involved in the regulation of apoptosis and cell growth were affected, including members of the JNK pathway, PPARG and RASSF1A, in addition to genes involved in the immune system.

Materials and methods

Sample cohort

Samples were collected from Children's Cancer and Leukaemia Group (CCLG) and the Cooperative Human Tissue Network (CHTN). Ninety-eight snap-frozen ependymoma samples were used in the methylation profiling, including 73 primary and 25 recurrent tumors. Primary and subsequent recurrent tumor samples were used from nine patients. The cohort also contained 12 recurrent tumors from nine patients with no paired primary sample. The mean and median age of the cohort was 6.8 and 6 years, respectively. Of the primary tumors 53% were posterior fossa, 23% supratentorial and 15% spinal. Data were unavailable for six tumors. After central histopathological review of 72/73 primary tumors, 7% were grade I, 52% grade II and 40% grade III. One tumor was acquired after central review. Local review classed the tumor as grade II/III. Of the grade I tumors, all were myxopapillary spinal ependymomas.

Clinical information was obtained from the CCLG, CHTN and local centers. Multiple Centre Research Ethics Committee (MREC) approval was obtained for the study. Consent for use of tumor samples was taken in accordance with national tumor banking procedures and the Human Tissue Act. Work was conducted in premises licensed under the Human Tissue Act.

DNA extraction

Prior to DNA extraction, a small piece of tissue was prepared on a slide as a diagnostic smear with subsequent hematoxylin and eosin staining. The slides were reviewed by a pathologist to determine if tumor cells were present. DNA was extracted from 10 mg of tissue. DNA was also extracted from the neural stem cell line ReNcell VM (Millipore), using 1 million cells per extraction. Each sample was lysed in lysis buffer (50 mM Tris pH 8, 100 mM EDTA pH 8, 100 mM NaCl, 1% SDS) and proteinase K (20 mg/ml) at 37°C overnight. DNA was obtained by phenol:chloroform extraction followed by isopropanol precipitation. DNA quality was checked by electrophoresis of 1 μl of sample through a 1% agarose gel at 120 V.

Methylation array analysis

DNA from 98 ependymoma samples plus three replicates of the ReNcell VM cell line was processed using the GoldenGate® Cancer Panel I assay for methylation (Illumina) at the Wellcome Trust Centre for Genetics, Oxford, UK, according to manufacturer's instructions. In brief, 500 ng genomic DNA from each sample underwent bisulphite conversion. Half of the sample was then used in the GoldenGate® assay. Following hybridization and washing, slides were scanned using the Illumina Beadarray™ Reader. Initial data quality control measures were undertaken using Beadstudio v.32 methylation module™

(Illumina). Probes with aberrant signal intensity were identified using a calculated probe detection value. Samples were excluded from further analysis if more than 1% of the 1,505 probes had a detection p value greater than 0.05. Spatial artifacts were identified using the Beadarray Subversion of Harshlight (BASH) [8] feature within the beadarray package (http://www.bioconductor.org). Samples with significantly large spatial defects, greater than 25% of the array area, were excluded from further analysis.

Data analysis was undertaken in R and Bioconductor®. After background signal correction, a beta value was attributed to each measured probe, representing the level of methylation, with values ranging from zero (unmethylated) to one (hypermethylated). Before downstream analysis, probes from the X chromosome were removed. Bootstrapped unsupervised hierarchical clustering was performed using the R package 'pvclust' [61], using Euclidean distance, average agglomeration and 10,000 replications. The observed cluster patterns were verified using principal component analysis using the 'rgl', 'pvclust' and 'cluster' packages.

Statistical comparisons were performed in GeneSpringGX 11.0 (Agilent, Santa Clara, Ca, USA). Genes showing significantly different methylation levels between groups were identified using a Kruskal–Wallis test with a Benjamini and Hochberg multiple test correction [4]. Genes were considered significant if their p value was less than 0.05. Additional genes were removed if the difference in average beta values between groups was less than 0.34. Identified gene lists were analyzed using the online functional annotation tool DAVID [25, 26] and Ingenuity Pathway Analysis (IPA) 9.0 (http://www.ingenuity.com).

To determine global levels of hypo- or hypermethylation the number of probes with beta values less than or equal to 0.2 (hypomethylation), or values greater than or equal to 0.8 (hypermethylation) were calculated. The numbers calculated for each group were compared using a t-test to identify significant differences.

Bisulphite sequencing

Seventeen tumors that had been run on the methylation arrays were further analyzed by bisulphite sequencing. One sample was a recurrence, the rest primary tumors. Five tumors were supratentorial, three spinal, and nine posterior fossa.

1 µg DNA from each sample was bisulphite converted using the CpGenome DNA modification kit (Millipore, Billerica, MA, USA). Primers were designed to amplify a product, from bisulphite modified DNA, covering the selected methylation loci (Online Resource 1). PCR reactions were carried out by incubating bisulphite modified DNA with 1.25 U of platinum taq (Invitrogen, Carsbad,

CA, USA), 8.3 mM dNTPs, 2 mM $MgCl_2$ and forward and reverse primers (1 µM). Optimized levels of betaine and DMSO were added to reactions for specificity (Online Resource 1). PCR conditions were; 95°C for 5 min followed by 40 cycles of 95°C for 30 s, an annealing temperature specific to each primer pair (Online Resource 1) for 1 min and 72°C for 1 min. This was followed by a final extension step at 72°C for 10 min.

PCR products were purified by incubation with 0.3 U shrimp alkaline phosphatase (Promega, Madison, WI, USA) and 1.5 U exonuclease I (NEB, Ipswich, MA, USA) at 37°C for 8 min, followed by 15 min at 72°C. Sequencing reactions were undertaken by Source Bioscience (Nottingham, UK). Sequences were analyzed using Mutation Surveyor v3.97 (SoftGenetics, PA, USA). The level of methylation was represented by the percentage of cytosine, calculated using the simplified allele ratio function.

Expression array analysis

Previously published ependymoma mRNA expression data were used [28]. Ten samples from this study were run on the methylation arrays in our study which included eight primary tumors, and a second and third recurrent sample from one patient. Five of the samples were supratentorial and five located in the posterior fossa. Data analysis was initially undertaken using GeneSpringGX 11.0 (Agilent). Raw data (CEL files) downloaded from Gene Expression Omnibus (GEO) under the accession number GSE21687 were processed using the robust multiarray average (rma) algorithm. A number of the tumors used in this study were from adult patients. These were excluded from comparisons to our methylation data on pediatric ependymomas. Previously published normal fetal brain regional expression data were additionally analyzed [41]. MAS5 processed data were downloaded from GEO (accession number GSE1397).

Genes differentially expressed between groups were identified using an ANOVA test with a Benjamini and Hochberg multiple test correction [4]. Genes were considered significant if their p value was less than 0.05. Identified gene lists were analyzed using IPA. A comparison between methylation and expression array data, for genes showing significant differential methylation between tumor location groups, was analyzed for the 10 samples run on both array platforms using Pearson's correlation in SPSS (IBM, NY, USA).

Quantitative PCR

Total RNA was extracted from 19 ependymoma frozen tumor samples. Fifteen were primary tumors and four were recurrences. Twelve were posterior fossa, five supratentorial and two spinal. 40–50 mg of tissue were used for

extraction using the mirVana™ miRNA Isolation kit (Applied Biosystems, Carlsbad, CA, USA). After extraction RNA was treated with DNase (Promega) (2 U) at room temperature for 15 min. cDNA synthesis was carried out by incubating 500 ng RNA with 200 U reverse transcriptase (Fermentas, St. Leon-Rot, Germany) at 42°C for 1 h. Reactions were terminated by incubating at 70°C for 5 min. A control was included for each sample where reverse transcriptase was excluded from the reaction mix to test for genomic DNA contamination in subsequent PCR reactions.

Primer sequences for quantitative PCR (qPCR) are given in Online Resource 1. PCR reactions were carried out by incubating an equivalent of 8.3 ng of starting RNA with 1Q Custom SYBR Green Supermix (BIO-RAD, Hercules, CA, USA) and forward and reverse primers (100 nM). The CFX96 real time PCR machine (BIO-RAD) was used. PCR conditions were; 95°C for 10 min followed by 40 cycles of 95°C for 30 s, an annealing temperature specific to each primer pair (Online Resource 1) for 1 min and 72°C for 1 min. This was followed by a dissociation (melting curve) analysis. Data were normalized using GAPDH. Each cDNA sample was analyzed in triplicate. Primer efficiency and precision were calculated using a standard curve. Relative expression to a calibrator sample (fetal brain or selected tumor sample) was calculated using the Pfaffl equation [54].

Results

Hypermethylated profile identified based on tumor location

Methylation array data were generated for 98 ependymoma samples including 73 primary tumors and 25 recurrences. The data were initially analyzed by unsupervised hierarchical clustering and principal component analysis (Fig. 1). Tumors mainly grouped according to location, separating into groups arising in supratentorial, posterior fossa and spinal regions of the CNS. No other factor displayed an association with the cluster groups. Survival analysis revealed no significant differences in patient outcome between cluster groups (data not shown).

Eighty-four probes, representing 70 genes, showing significant differences in methylation levels between tumors from different locations were identified using a Kruskal–Wallis test (Online Resource 2). No significant differences were found when clinical groups, including age at diagnosis, patient sex and tumor grade, were compared. Additionally no differences were identified between primary and recurrent tumors.

We noted that a high proportion of the genes displaying location-based methylation differences were hypermethylated in supratentorial and spinal tumors (75%) and hypomethylated in posterior fossa tumors (25%) (Fig. 2a, b). To investigate this further we compared the numbers of probes in each group which were totally unmethylated (beta value ≤ 0.2) or totally methylated (beta value ≥ 0.8). Posterior fossa tumors displayed a significantly higher number of probes with no methylation (p value 0.0005) and a significantly lower number of probes with complete methylation (p value 0.0009). This hypermethylated phenotype, seen in supratentorial and spinal ependymomas, was also reflected at the expression level. Using an independent mRNA expression array dataset, originally published by Johnson et al. [28] (Geo accession number GSE21687), we found more genes, across the whole array, displayed up-regulated expression in posterior fossa tumors compared to supratentorial and spinal (Fig. 2c).

Genes encoding for proteins involved in the methylation of DNA, including the DNA methyltransferases DNMT1, DNMT3A and DNMT3B, displayed statistically significant differential expression in posterior fossa tumors compared to supratentorial and spinal tumors (Fig. 3). Most genes in this pathway displayed up-regulated expression in supratentorial and spinal tumors, suggesting the de-regulated expression of components of the methylation machinery may be the mechanism by which the hypermethylated profile is being generated.

Identification of candidate genes

Genes with significant differences in methylation levels between tumors from different locations (Online Resource 2) were analyzed using the online functional annotation tool DAVID [25, 26]. Genes identified included those involved in the regulation of apoptosis and cell growth. The growth regulator PPARG was methylated in supratentorial and spinal tumors. Genes involved in apoptosis included TP73, which was methylated in supratentorial tumors, and HDAC1, which was methylated in spinal tumors. The tumor suppressor gene RASSF1A displayed hypermethylation in all intracranial tumors. Members of the MAPKKK cascade and the JAK/STAT pathway were also significantly enriched. This included members of the c-Jun N-terminal kinase (JNK) signaling pathway; MAPK10 and MAP3K1 which displayed hypermethylation in supratentorial and spinal tumors. A relatively low number of genes displayed hypermethylation in posterior fossa tumors. Genes in this group included IRF7, FABP3 and CRIP1.

Further analysis using IPA identified significant enrichment for signaling pathways including DNA methylation and transcriptional repression signaling, JNK signaling, PPAR signaling, death receptor signaling, JAK/STAT signaling and TGFB signaling (Online Resource 3). Many pathways involving the innate and adaptive immune
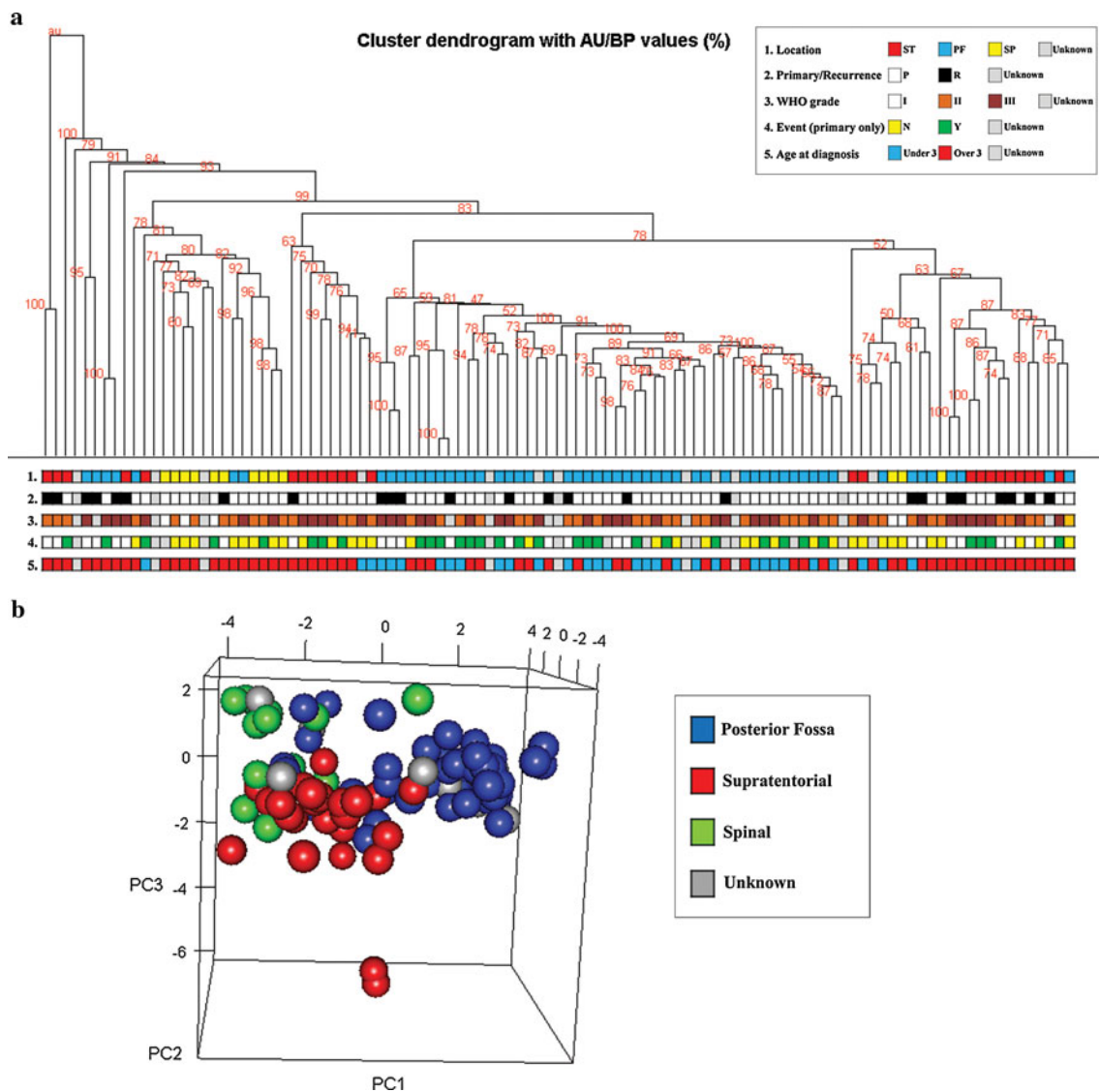
Fig. 1 **a** Hierarchical clustering dendogram of ependymomas using all methylation probes. Clustering was carried out using the 'pvclust' package in R. AU *p* values are displayed in *red*. Tumors grouped according to location in the CNS. Other clinical factors including WHO grade, age at diagnosis, whether a sample was a primary or recurrent tumor and whether patients with a primary tumor had a subsequent event (recurrence or death) are displayed. No other factor displayed an association with the cluster groups. **b** The segregation of tumors arising in different locations was confirmed using principal component analysis

system, particularly cytokine signaling, also displayed significant enrichment.

Analysis at the gene expression level revealed correlations with the methylation data

To identify which methylation alterations induced mRNA expression level changes we again analyzed ependymoma expression array data originally published by Johnson et al. [28]. Methylation and expression array data were directly compared for 10 tumor samples which were run on both array platforms. A Pearson's correlation was calculated for the genes which displayed significant differential methylation between tumors from different locations. Seventeen out of 84 (20%) probes, representing 16 genes, displayed a significant inverse correlation (Table 1).

We additionally identified genes showing differential expression between tumors arising in supratentorial, posterior fossa or spinal locations across the whole cohort analyzed on the mRNA expression arrays (Online Resource 4). Out of the genes identified in the methylation analysis, 40% also displayed a significant difference in mRNA expression. The expression levels for approximately half of these genes displayed an inverse pattern to that found in the methylation data, suggesting methylation was directly influencing mRNA expression (Table 2).
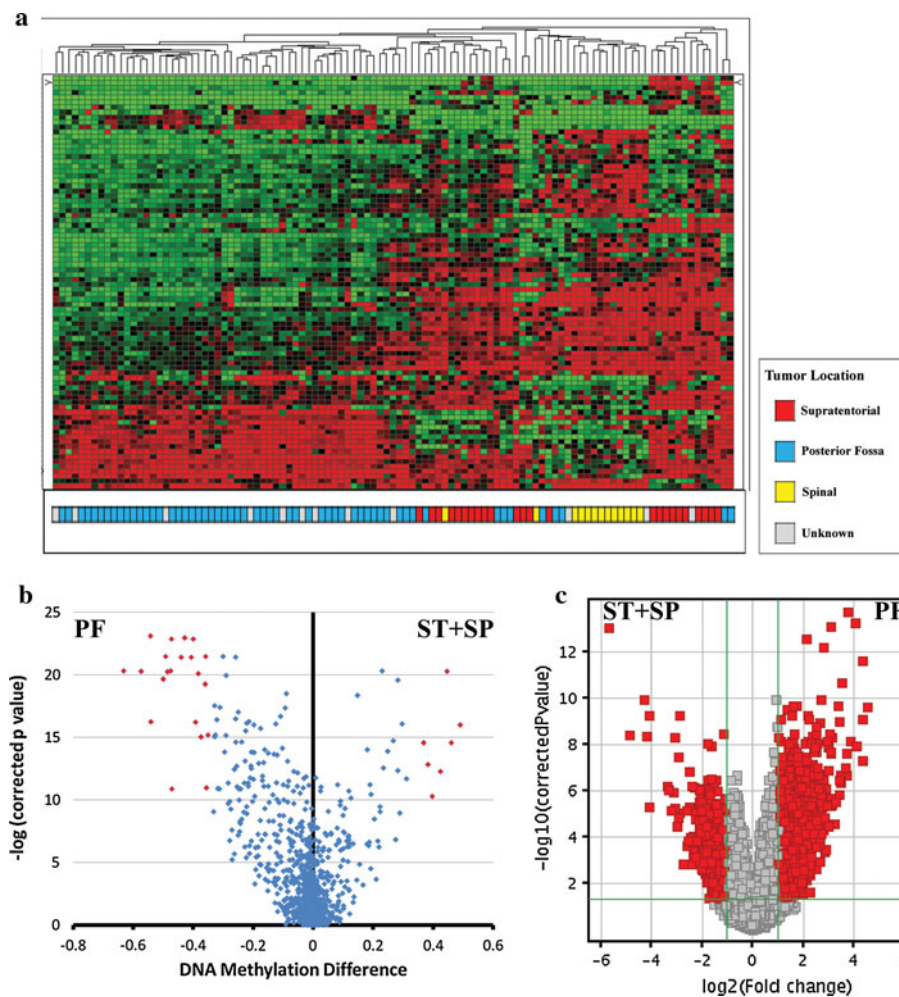
Fig. 2 Hierarchical clustering of probes displaying significant differences in methylation between tumors from different locations (**a**). On the heat map *red boxes* represent high beta values and *green* low beta values. Posterior fossa (*PF*) tumors formed a separate cluster to the rest of the tumors and displayed fewer hypermethylated (*red*) probes compared to supratentorial (*ST*) and spinal (*SP*) tumors. The difference in the level of hypermethylation is also illustrated in a volcano plot (**b**). The negative logged *p* value (Kruskal–Wallis test) is displayed along the *y*-axis. The difference in average beta values between the posterior fossa vs the supratentorial and spinal tumors is displayed along the *x*-axis. Probes with a significant *p* value (<0.05) and a difference in beta value greater than 0.34 are highlighted in *red*.

A greater number of probes were hypomethylated in posterior fossa tumors (negative DNA methylation difference). The methylation phenotype seen was reflected at the mRNA expression level illustrated by a volcano plot (**c**). A global comparison using all probes on the array was undertaken comparing posterior fossa to supratentorial and spinal tumors. The negative log *p* value (*t*-test PF vs. ST + SP) is displayed along the *y*-axis and the logged fold change [PF/(ST + SP)] along the *x*-axis. Probes with a significant *p* value (<0.05) and a fold change greater than two are highlighted in *red*. A greater number of probes were up-regulated in posterior fossa ependymomas (positive fold change) compared to supratentorial and spinal tumors

Eight out of the 16 genes which displayed an inverse correlation between methylation and expression levels for the 10 ependymomas analyzed on both array platforms also displayed significant differential mRNA expression across the whole cohort.

Genes identified included those involved in the control of cell growth and death such as MAPK10 and PPARG. A number of genes involved in the immune response were also found including NOD2, IRF7, IRAK3, OSM and PI3. As only a small number of spinal tumors were included in the mRNA expression analysis it was difficult to identify

which genes correlated with the methylation data in this group.

We analyzed the location based mRNA gene lists identified in the statistical analysis using IPA. One-third of canonical pathways identified in the methylation analysis were also enriched for at the mRNA expression level (Online Resource 5). Many of the pathways that overlapped were involved in cell death and the immune response. Analysis demonstrated that a number of genes from the JNK signaling pathway displayed differential expression between tumors arising in different CNS locations (Fig. 4).

Fig. 3 Expression differences in genes involved in DNA methylation and transcriptional repression signaling were seen between ependymomas from different CNS locations. The figure illustrates expression differences between supratentorial and posterior fossa tumors only as very few spinal tumors were analyzed at the mRNA expression level. Genes highlighted in *green* represent those with higher expression in supratentorial tumors and genes in *pink* those with higher expression in posterior fossa tumors. The majority of genes displayed higher expression in supratentorial tumors. The image in the figure was taken from IPA
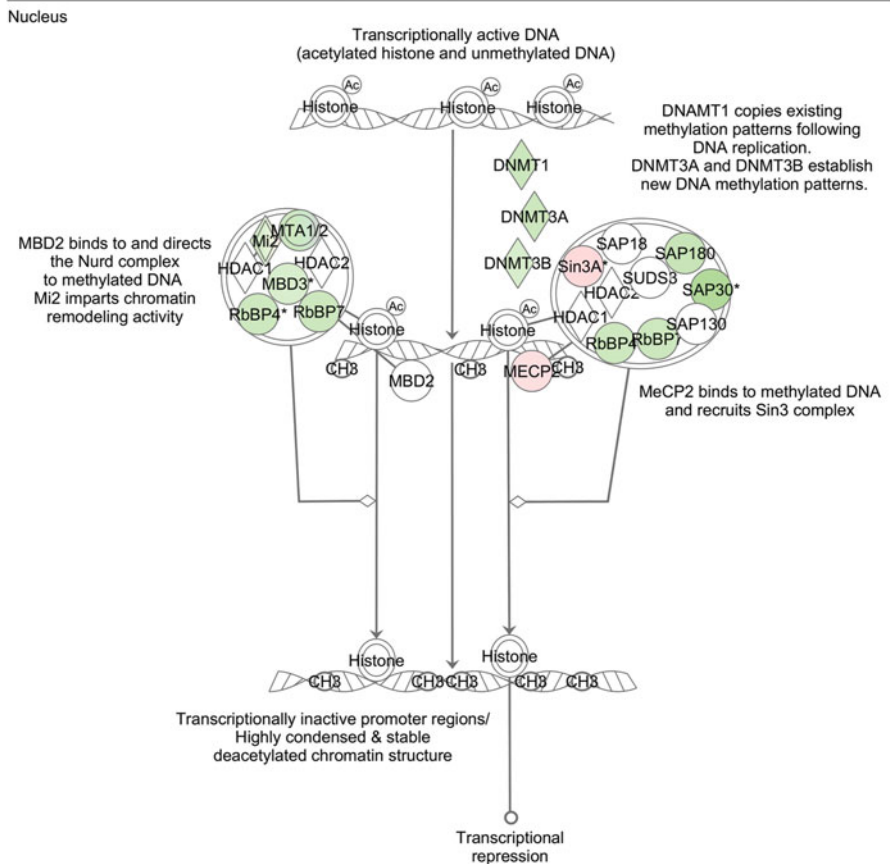
Validation of selected candidate genes

The methylation status of six genes; MAPK10, PPARG, FABP3, EYA4, CRIP1 and IRF7 was validated using bisulphite sequencing. Genes displaying hypermethylation in each location tumor group, which also displayed an inverse correlation at the mRNA expression level, were chosen. The pattern of methylation identified by bisulphate sequencing significantly correlated with the array data (Fig. 5). Adjacent CpGs also displayed a significant correlation with the validated CpG for the majority of genes analyzed (data not shown).

The mRNA expression of the same six genes was validated using qPCR. All genes displayed a similar pattern of expression to the mRNA expression array data and an inverse pattern to the methylation array data (Online Resource 6).

Comparison to normal brain

Previous studies have demonstrated differences in the level of methylation between regions of the adult brain [20, 34]. This could suggest that the segregation of the ependymomas according to location that we found could have been affected by "contaminating" surrounding brain tissue. We checked for the presence of normal tissue using H and E stained smears of the tumor samples. However, this only analyzed a small piece of the tissue used. The study by Ladd-Acosta et al. [34] demonstrated significant differences in methylation between adult cerebral cortex and cerebellum using the same array platform as we used in our study. We compared their gene list to genes showing significant differences in methylation between supratentorial and posterior fossa ependymomas (Online Resource 7). Using the same stringency cut offs, only two genes, LCN2 and WRN2, were found on both lists. Additionally, a similar percentage of genes were hypermethylated in each normal brain region (cerebral cortex 60%, cerebellum 40%) compared to the supratentorial bias observed in the ependymomas (supratentorial 79%, posterior fossa 21%).

We were unable to obtain methylation data for fetal brain regions. Therefore, we looked at RNA expression, using a previously published dataset (GEO accession GSE1397) [41]. In ependymoma, we found that approximately 20% of genes differentially methylated between location groups displayed an inverse pattern of mRNA expression. If the differences in methylation were due to "contaminating" normal tissue we would expect to see a

Table 1 Genes displaying a significant correlation between methylation and mRNA expression array data for the 10 ependymomas analyzed on both array platforms

Gene	Methylation probe ID	Expression probe ID	Pearson's correlation (r)	p value
NAT2	NAT2_P11_F	206797_at	−0.894	<0.001
NOD2	CARD15_P302_R[a]	220066_at	−0.922	<0.001
PPARG	PPARG_P693_F	208510_s_at	−0.938	<0.001
IRF7	IRF7_E236_R	208436_s_at	−0.793	0.006
	IRF7_P277_R	208436_s_at	−0.866	0.001
CHI3L2	CHI3L2_E10_F	213060_s_at	−0.783	0.007
MAPK10	MAPK10_E26_F	204813_at	−0.778	0.008
OSM	OSM_P34_F	230170_at	−0.743	0.014
EYA4	EYA4_P794_F	207327_at	−0.707	0.022
		238877_at	−0.737	0.015
TAL1	TAL1_E122_F	1561651_s_at	−0.732	0.016
IRAK3	IRAK3_P185_F	213817_at	−0.725	0.018
HDAC1	HDAC1_P414_R	201209_at	−0.694	0.026
PI3	PI3_P1394_R	203691_at	−0.674	0.033
		41469_at	−0.695	0.026
RBP1	RBP1_P426_R	203423_at	−0.687	0.028
CRIP1	CRIP1_P874_R	205081_at	−0.686	0.029
BCR	BCR_P346_F	202315_s_at	−0.682	0.030
		217223_s_at	−0.639	0.047
TJP2	TJP2_P518_F	202085_at	−0.673	0.033

[a] CARD15 was renamed as NOD2

similar overlap with normal fetal brain. We identified genes with significantly different RNA expression between cerebrum and cerebellum samples using a *t*-test (Online Resource 8). We found that none of the genes we identified to be differentially methylated between supratentorial and posterior fossa ependymomas (Online Resource 7) showed significantly different mRNA expression between normal fetal brain regions. These results suggest the differences we found are tumor specific and not due to "contaminating" normal tissue.

Previous studies have shown similarities between ependymoma expression profiles and those of neural stem cells [28, 62]. We therefore compared our methylation profiles to those from the fetal neural stem cell line ReN-cell VM. Hierarchical clustering and PCA, using the genes which displayed significant methylation differences between the ependymomas from different locations, showed the neural stem cells grouped with the supratentorial and spinal ependymomas (Fig. 6). Statistical comparisons between tumors from different locations and the neural stem cells showed that only the posterior fossa tumors displayed a relatively large number of significant differences (Online Resource 9). Only one gene, DUSP4, displayed a significant difference in methylation level between supratentorial ependymomas and neural stem cells, being more methylated in the stem cells. No significant differences were found between spinal tumors and neural stem cells.

Discussion

We have analyzed a large cohort of ependymomas to identify alterations in methylation across the genome. Through an integrated analysis with ependymoma mRNA expression array data we have identified global changes in methylation patterns and specific candidate genes and pathways that may be involved in tumor pathogenesis. Our analysis suggests epigenetic silencing of tumor suppressor genes, through DNA methylation, is an important mechanism in the pathogenesis of supratentorial and spinal ependymomas.

As previously shown with DNA copy number and mRNA expression data [28, 62], we observed location based differences at the level of methylation. Our analysis revealed a global difference in the methylation levels between tumors arising in different regions of the CNS. Ependymomas from supratentorial and spinal locations displayed significantly more hypermethylated genes than tumors from the posterior fossa region, suggesting this may be an important mechanism of tumor suppressor gene inactivation in supratentorial and spinal but not posterior

Table 2 Genes displaying significant differences in mRNA expression between tumors from different CNS locations that were also identified in the methylation analysis

Probe set ID	Corrected *p* value	Regulation ((PF) vs. (SP))	Regulation ((PF) vs. (ST))	Regulation ((SP) vs. (ST))	Gene symbol
208510_s_at	*4.58E−07*	*Up*	*Up*	*Up*	*PPARG*
204379_s_at	1.02E−06	Up	Down	Down	FGFR3
204380_s_at	2.69E−04	Up	Down	Down	FGFR3
204813_at	*2.64E−05*	*Up*	*Up*	*Up*	*MAPK10*
206797_at	0.001860389	Down	Up	Up	NAT2
213060_s_at	0.002203304	Up	Up	Down	CHI3L2
239782_at	0.003380862	Up	Up	Up	RBP1
203423_at	0.019743502	Down	Up	Up	RBP1
208436_s_at	0.007062891	Down	Down	Up	IRF7
226602_s_at	0.011980913	Up	Up	Up	BCR///FLJ42953///LOC100133163/// LOC728468
213441_x_at	0.012686884	Up	Up	Down	SPDEF
214403_x_at	0.040593553	Up	Up	Down	SPDEF
213442_x_at	0.048410457	Up	Up	Down	SPDEF
214404_x_at	0.038640525	Up	Up	Down	SPDEF
205738_s_at	0.013991439	Up	Down	Down	FABP3
238877_at	*0.037761625*	*Down*	*Up*	*Up*	*EYA4*
208568_at	0.039600316	Up	Up	Down	MC2R
205168_at	0.040356502	Up	Down	Down	DDR2

Only the genes which displayed an inverse pattern to the methylation data are listed. Probes that are italicized represent genes which also displayed a significant inverse correlation between the methylation and expression data for the tumor samples run on both array platforms (Table 1)

*PF* posterior fossa, *ST* supratentorial, *SP* spinal

fossa ependymomas. This was reflected at the mRNA expression level. A larger proportion of genes displaying tumor location differences in expression were up-regulated in posterior fossa tumors compared to ependymomas from other CNS locations. Normally most gene promoters are unmethylated [29]. However, increased methylation of CpG islands in the promoter regions of a large number of genes has been seen in a variety of cancers. A 'CpG island methylator phenotype' (CIMP) was originally described in a subset of colon carcinomas [63, 67]. The same methylator phenotype has also been described in glioma [35, 49]. In some cancers a hypermethylated phenotype has been associated with poor outcome [27]. However, in glioma the 'methylator' subgroup was linked to a better prognosis [49]. We did not find an association between methylation and survival.

Without an appropriate normal control it cannot be concluded whether the hyper- or hypomethylation profiles are closer to normal for ependymoma. A recent study of the methylation levels of CpG sites within or flanking alu elements in ependymoma identified a global loss in methylation which was associated with more aggressive or recurrent tumors [69]. In our study, we found no significant differences in methylation between primary and recurrent

tumors. However, in the study by Xie et al. loci exhibiting a significant loss of methylation tended to be further from transcription factor binding sites suggesting they were different to the CpG sites included in our analysis, which were designed to be in the vicinity of gene promoters. In cancer, hypermethylation within gene promoters is more common than hypomethylation. The latter is more frequently found in intergenic regions [13, 19, 44, 56]. This suggests the hypermethylation we found in supratentorial and spinal tumors is more likely to be the aberrant profile.

The methylation and expression data both suggested the underlying mechanism behind the global hypermethylation seen in supratentorial and spinal ependymomas may be due to deregulation of the DNA methylation machinery. Over expression of genes involved in the methylation of DNA has been seen in other cancers and has been associated with CpG hypermethylation [47]. In contrast, loss of expression of these genes has also been associated with global hypomethylation [18, 47].

Reducing hypermethylation therapeutically may be a promising approach in the treatment of some cancers. Hypomethylation therapies have been approved for use in liquid tumors [29]. However, these therapies risk activating methylated oncogenes. Further analysis is needed to
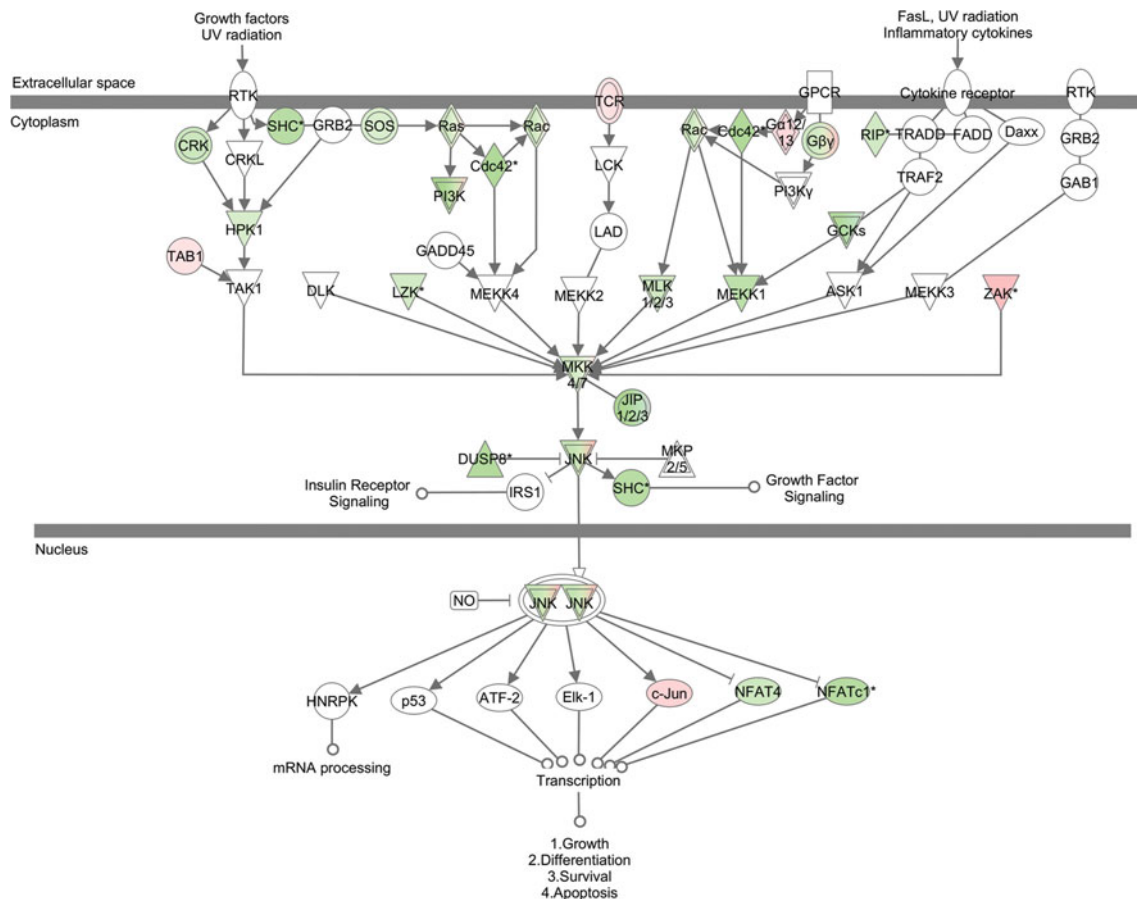
Fig. 4 Significant differences in mRNA expression were seen for genes involved in the JNK signaling pathway between tumors arising in different CNS locations. The figure illustrates expression differences between supratentorial and posterior fossa tumors only as very few spinal tumors were analyzed at the mRNA expression level. Genes highlighted in *green* represent those with higher expression in supratentorial tumors and genes in *pink* those with higher expression in posterior fossa tumors. The majority of genes displayed higher expression in supratentorial tumors. However, MAPK10 (JNK3) and the downstream target c-Jun displayed higher expression in posterior fossa tumors. The image in the figure was taken from IPA

determine the importance of the hypermethylation seen in ependymoma to determine how effective hypomethylation therapies would be.

Our data suggested that, at the DNA methylation level, supratentorial and spinal ependymomas displayed more similarities than supratentorial and posterior fossa tumors. This is somewhat surprising as spinal ependymomas differ clinically, being much rarer in children and having a better prognosis than intracranial tumors [38, 45]. Spinal tumors also display a distinct copy number profile from supratentorial tumors, characteristically showing gains or losses of large genomic regions compared to supratentorial tumors which display more focal alterations [28]. Spinal tumors also display significant differences in mRNA expression compared to intracranial tumors [62].

Tumors could also segregate according to location if "contaminating" surrounding brain tissue was biasing the results. Our meta-analysis of normal adult brain methylation and fetal brain expression data suggests this is not the

case. The genes displaying differences between samples from supratentorial and posterior fossa locations were not the same as the differences seen in the tumor samples suggesting the methylation patterns are tumor specific.

Studies have suggested ependymomas found in different locations within the CNS arise from distinct progenitor cell populations [28]. The RNA expression patterns of supratentorial ependymomas was shown to resemble mouse neural stem cells isolated during embryonic development and spinal tumors that of adult mouse neural stem cells, suggesting the tumors had retained or recapitulated the expression profile of these stem cells. Our analysis demonstrated that human fetal neural stem cells displayed a similar methylation pattern to supratentorial tumors supporting this hypothesis. All the spinal tumors we analyzed were pediatric which may explain why we found them to be similar to fetal neural stem cells in contrast to Johnson et al. who found spinal tumors to be more similar to adult cells. The published study by Johnson et al. mainly
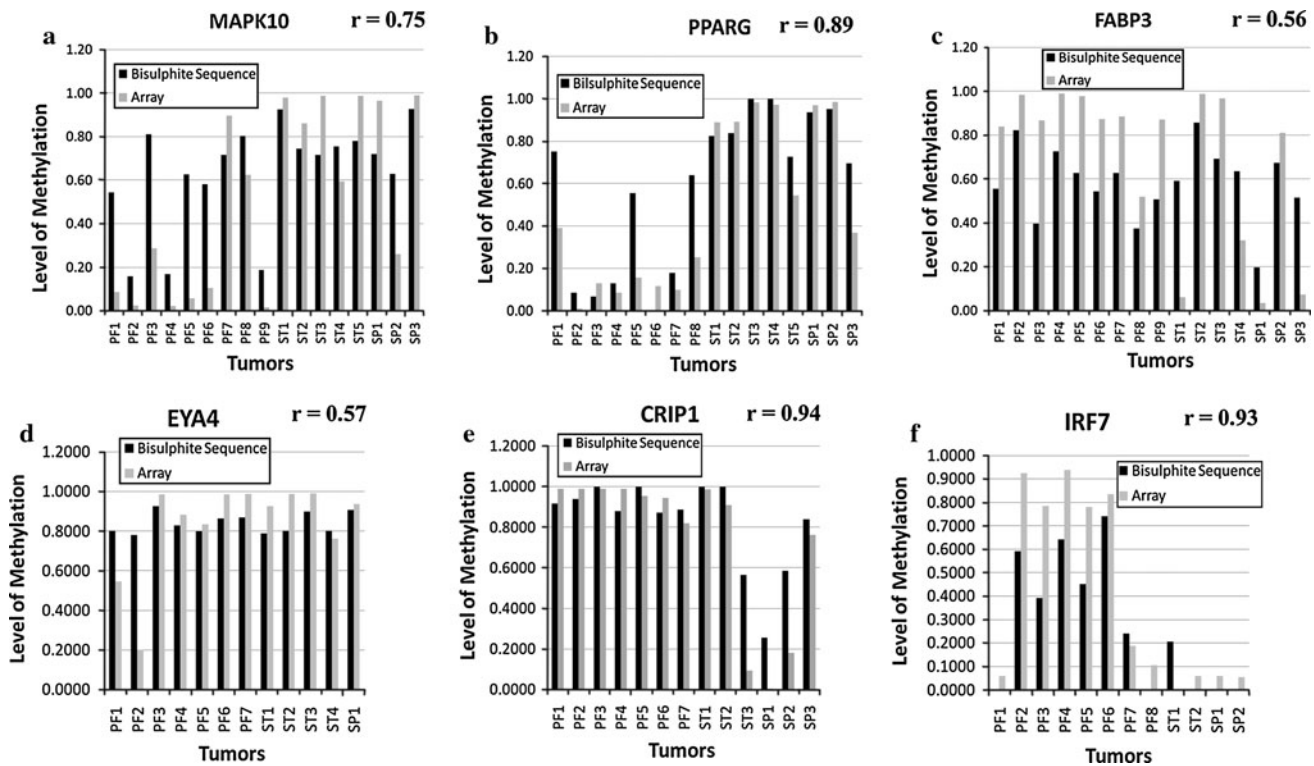
Fig. 5 Methylation levels measured by bisulphite sequencing and the methylation array displayed a significant correlation for the selected genes. **a** MAPK10 (Pearson's $r = 0.75$, $p = 0.0004$), **b** PPARG (Pearson's $r = 0.89$, $p = 3 \times 10^{-6}$), **c** FABP3 (Pearson's $r = 0.56$, $p = 0.026$), **d** EYA4 (Pearson's $r = 0.57$, $p = 0.053$), **e** CRIP1 (Pearson's $r = 0.94$, $p = 1.4 \times 10^{-6}$), **f** IRF7 (Pearson's $r = 0.93$, $p = 1.4 \times 10^{-5}$). Tumors are labeled on the *x*-axis; *PF* posterior fossa, *ST* supratentorial, *SP* spinal. For the bisulphite sequencing data the level of methylation is represented by the percentage of cytosine. For the array data the methylation level is represented by the beta value

comprised adult spinal ependymomas. The neural stem cells we analyzed were derived from the ventral mesencephalon of fetal brain tissue. It may be that posterior fossa tumors arise from stem or progenitor cells from a different location.

It has been reported that cell lines display increased methylation compared to uncultured cells [60]. The neural stem cell line we used was also immortalized using v-myc which could potentially alter the methylation profile from that of the original cells. However, it has been demonstrated that the immortalized cells behave like the original stem cells and retain a normal karyotype even after many passages [15]. Additionally, the similarity we found between the methylation profiles of the neural stem cells and spinal and supratentorial ependymomas is unlikely to have occurred by chance.

Integration of methylation and mRNA expression data allowed us to identify methylation-induced gene expression changes. Most notably, we identified many genes involved in the control of cell growth and death and pathways involved in the immune system. Only 20% of genes displayed an inverse correlation between methylation and expression data. This is consistent with previous cancer studies [24, 49, 55]. Methylation can only control the potential for gene expression. Therefore, if the signal to induce expression is not present no gene expression will be detected irrespective of methylation status. Additionally, the array only measured a specific subset of CpG islands. Methylation of additional adjacent CpGs may be needed to down regulate expression of some genes.

Increased methylation of genes in the JNK signaling pathway, including MAPK10 and MAP3K1, were seen in supratentorial and spinal tumors. This pathway can induce apoptosis under stress conditions such as exposure to inflammatory cytokines or environmental factors including chemotherapeutic drugs [14]. MAPK10 gene expression inversely correlated with methylation levels. This gene has been found to be methylated in a number of cancers including glioma [35, 72]. MAPK10 expression has also been shown to be lost in brain tumor cell lines [73]. In the human body MAPK10 expression is restricted to specific organs including the brain [33, 42]. Functional studies have shown that in a MAPK10 knockout mouse, hippocampal neurons are resistant to glutamate induced excitotoxicity suggesting a role for signaling through MAPK10 in neuronal cell death [32, 71].
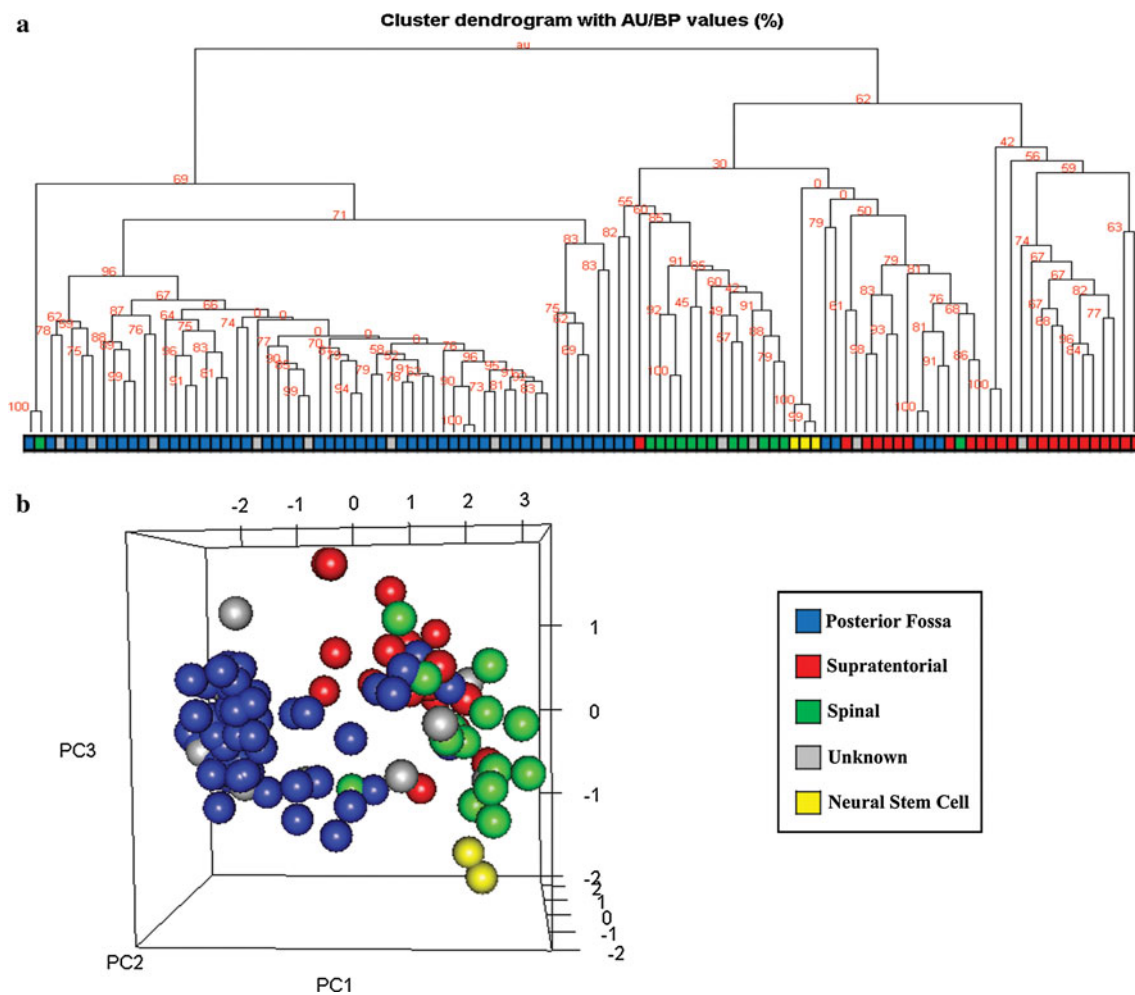
Fig. 6 Hierarchical clustering of all ependymomas and the fetal neural stem cell line ReNcell VM, using only probes that displayed a significant difference in methylation between ependymomas from different locations (**a**). Clustering was carried out using the 'pvclust' package in R. AU *p* values are displayed in *red*. The neural stem cells segregated with supratentorial and spinal tumors. These groupings were confirmed using principal component analysis (**b**)

At the expression level we found the majority of genes involved in the JNK pathway to be up-regulated in supratentorial tumors. However, these genes were all upstream of MAPK10. The downstream target of MAPK10, JUN, displayed decreased expression in supratentorial tumors, as seen for MAPK10 itself. This may suggest that the pathway is being activated in supratentorial tumors to induce cell death. However, inactivation of MAPK10 by DNA methylation inhibits this process.

PPARG was hypermethylated in supratentorial and spinal tumors relative to posterior fossa tumors. An inverse correlation was seen at the mRNA expression level in our analysis and in a previous study [62]. PPARG is a transcription factor that plays a role in many physiological processes including cell growth. The gene has been implicated in many cancers including colon cancer where reduced expression through hypermethylation was associated with progression and an adverse outcome [53].

Treatment of glioma cells in vitro and in vivo with PPARG agonists decreased cell growth and induced apoptosis [3, 11, 21]. If a similar effect is seen in ependymoma this may be a potential therapeutic target.

We found the tumor suppressor gene RASSF1A to be hypermethylated in intracranial ependymomas. This gene has been shown to be methylated in a large number of cancers including a high percentage of ependymomas [1, 22, 46]. RASSF1A has a large number of functions including a role in regulating cell cycle progression and induction of apoptosis [57]. Other genes involved in apoptosis, identified in our analysis, included TP73 and HDAC1. TP73, which was hypermethylated in supratentorial tumors, has also been shown to be methylated in ependymoma previously [2, 22]. It has been shown to induce apoptosis in conjunction with RASSF1A [43]. HDAC1 was found to be hypermethylated in spinal tumors.

EYA4 was hypermethylated in posterior fossa and supratentorial tumors. The gene encodes a member of the eyes absent protein family of transcription factors and plays a role in the development of the eye and inner ear in humans [7, 70]. It has previously been shown to be hypermethylated in other cancers, including colorectal cancer and Barrett's esophagus, suggesting a tumor suppressor role [50, 76]. We found an inverse correlation at the mRNA expression level which has also been found previously [62].

A relatively low number of genes were hypermethylated in posterior fossa ependymomas. FABP3 is a member of the intracellular lipid binding protein family. It binds fatty acids, plus other hydrophobic compounds, and regulates their physiological functions [37]. It may play a role in brain development as it is expressed in neurons [51]. IRF7 is a member of the interferon regulatory transcription factor family and plays a role in the transcriptional activation of virus inducible genes. It may also play a role in responding to cellular stresses such as DNA damage [31]. CRIP1 has been identified as a novel biomarker in cancers such as breast and cervical [9, 39]. It has also been shown to be hypomethylated in prostate cancer [65].

We identified a number of pathways involved in both the innate and adaptive immune system, particularly cytokine signaling, which displayed differential regulation between tumor groups. Many studies have demonstrated that a host immune response prevented tumor growth [17]. In ependymoma up-regulation of genes involved in the innate and adaptive immune response has been linked to a better outcome [16]. Although we did not find a link to outcome in our data analysis, methylation of genes involved in immunity may be one mechanism that suppresses the immune response in ependymoma. Methylation of genes involved in the immune system has also been seen in other cancers including melanoma [12]. Additionally, immune suppression has been shown to occur in different cancers including glioblastoma where it has been linked to tumor progression [59, 66].

A number of genes have been found to be methylated in ependymoma in previous studies. As discussed above we identified hypermethylation of RASSF1A and TP73 which have both been identified in previous research [2, 22, 46]. Our results also identified methylation of HIC1 and CASP8 agreeing with previous studies [22, 46, 64]. We found no evidence of methylation of CDKN2A, CDKN2B or MGMT which have all previously displayed hypermethylation in a proportion of ependymomas studied [22, 46, 58].

A study by Christensen et al. [10] analyzed the methylation status of 15 adult ependymomas. Comparison with adult temporal lobe identified hyper and hypomethylated genes. A small number of these genes were identified in our analysis, the majority of which were hypomethylated in

adult ependymomas and the posterior fossa tumors in our cohort. This included CHI3L2, TJP2, RBP1 and NAT2, which displayed an inverse correlation with mRNA expression in our study. Additionally RASSF1 was found to be hypermethylated as we found in all intracranial pediatric ependymomas. If adult and pediatric ependymomas have similar methylation profiles the results would suggest the tumors in the study by Christensen et al. were from the posterior fossa region. However, no location information was given. Genomically, pediatric and adult ependymomas have been shown to be different [30]. Additionally, normal fetal and adult brains show differences in methylation patterns [36, 74]. This would suggest pediatric and adult ependymoma may differ at the methylation level as well.

In conclusion, we have generated a global view of the methylation profile of ependymoma. Our data suggest that epigenetic silencing of tumor suppressor genes is an important mechanism in ependymoma pathogenesis in supratentorial and spinal tumors. Our integrated analysis has allowed us to identify candidate pathways and genes with potential methylation induced expression changes which may play a role in tumor pathogenesis.

Conflict of interest The authors declare that they have no conflict of interest.

References

1. Agathanggelou A, Cooper WN, Latif F (2005) Role of the Ras-association domain family 1 tumor suppressor gene in human cancers. Cancer Res 65:3497–3508

2. Alonso ME, Bello MJ, Gonzalez-Gomez P et al (2004) Aberrant CpG island methylation of multiple genes in ependymal tumors. J Neurooncol 67:159–165

3. Benedetti E, Galzio R, Cinque B et al (2008) Biomolecular characterization of human glioblastoma cells in primary cultures: differentiating and antiangiogenic effects of natural and synthetic PPARgamma agonists. J Cell Physiol 217:93–102

4. Benjamini Y, Hochberg Y (1995) Controlling the false discovery rate: a practical and powerful approach to multiple testing. J Roy Stat Soc B Methodol 57:289–300

5. Bestor TH (2000) The DNA methyltransferases of mammals. Hum Mol Genet 9:2395–2402

6. Bird AP, Wolffe AP (1999) Methylation-induced repression: belts, braces, and chromatin. Cell 99:451–454

7. Borsani G, DeGrandi A, Ballabio A et al (1999) EYA4, a novel vertebrate gene related to Drosophila eyes absent. Hum Mol Genet 8:11–23

8. Cairns JM, Dunning MJ, Ritchie ME, Russell R, Lynch AG (2008) BASH: a tool for managing BeadArray spatial artefacts. Bioinformatics 24:2921–2922

9. Chen Y, Miller C, Mosher R et al (2003) Identification of cervical cancer markers by cDNA and tissue microarrays. Cancer Res 63:1927–1935

10. Christensen BC, Smith AA, Zheng S et al (2011) DNA methylation, isocitrate dehydrogenase mutation, and survival in glioma. J Natl Cancer Inst 103:143–153

11. Cimini A, Cristiano L, Colafarina S et al (2005) PPARgamma-dependent effects of conjugated linoleic acid on the human glioblastoma cell line (ADF). Int J Cancer 117:923–933

12. Conway K, Edmiston SN, Khondker ZS et al (2011) DNA-methylation profiling distinguishes malignant melanomas from benign nevi. Pigment Cell Melanoma Res 24:352–360

13. Costello JF, Fruhwald MC, Smiraglia DJ et al (2000) Aberrant CpG-island methylation has non-random and tumour-type-specific patterns. Nat Genet 24:132–138

14. Davis RJ (2000) Signal transduction by the JNK group of MAP kinases. Cell 103:239–252

15. De Filippis L, Lamorte G, Snyder EY, Malgaroli A, Vescovi AL (2007) A novel, immortal, and multipotent human neural stem cell line generating functional neurons and oligodendrocytes. Stem Cells 25:2312–2321

16. Donson AM, Birks DK, Barton VN et al (2009) Immune gene and cell enrichment is associated with a good prognosis in ependymoma. J Immunol 183:7428–7440

17. Dunn GP, Old LJ, Schreiber RD (2004) The immunobiology of cancer immunosurveillance and immunoediting. Immunity 21:137–148

18. Eden A, Gaudet F, Waghmare A, Jaenisch R (2003) Chromosomal instability and tumors promoted by DNA hypomethylation. Science 300:455

19. Feinberg AP, Gehrke CW, Kuo KC, Ehrlich M (1988) Reduced genomic 5-methylcytosine content in human colonic neoplasia. Cancer Res 48:1159–1161

20. Gibbs JR, van der Brug MP, Hernandez DG et al (2010) Abundant quantitative trait loci exist for DNA methylation and gene expression in human brain. PLoS Genet 6:e1000952

21. Grommes C, Landreth GE, Sastre M et al (2006) Inhibition of in vivo glioma growth and invasion by peroxisome proliferator-activated receptor gamma agonist treatment. Mol Pharmacol 70:1524–1533

22. Hamilton DW, Lusher ME, Lindsey JC, Ellison DW, Clifford SC (2005) Epigenetic inactivation of the RASSF1A tumour suppressor gene in ependymoma. Cancer Lett 227:75–81

23. Hermann A, Gowher H, Jeltsch A (2004) Biochemistry and biology of mammalian DNA methyltransferases. Cell Mol Life Sci 61:2571–2587

24. Houshdaran S, Hawley S, Palmer C et al (2010) DNA methylation profiles of ovarian epithelial carcinoma tumors and cell lines. PLoS One 5:e9359

25. Huang da W, Sherman BT, Lempicki RA (2009) Bioinformatics enrichment tools: paths toward the comprehensive functional analysis of large gene lists. Nucleic Acids Res 37:1–13

26. Huang da W, Sherman BT, Lempicki RA (2009) Systematic and integrative analysis of large gene lists using DAVID bioinformatics resources. Nat Protoc 4:44–57

27. Issa JP (2003) Methylation and prognosis: of molecular clocks and hypermethylator phenotypes. Clin Cancer Res 9:2879–2881

28. Johnson RA, Wright KD, Poppleton H et al (2010) Cross-species genomics matches driver mutations and cell compartments to model ependymoma. Nature 466:632–636

29. Khin SS, Kitazawa R, Kondo T et al (2011) Epigenetic alteration by DNA promoter hypermethylation of genes related to transforming growth factor-b (TGF-b) signaling in cancer. Cancers 3:982–993

30. Kilday JP, Rahman R, Dyer S et al (2009) Pediatric ependymoma: biological perspectives. Mol Cancer Res 7:765–786

31. Kim TK, Kim T, Kim TY, Lee WG, Yim J (2000) Chemotherapeutic DNA-damaging drugs activate interferon regulatory factor-7 by the mitogen-activated protein kinase kinase-4-cJun NH2-terminal kinase pathway. Cancer Res 60:1153–1156

32. Kuan CY, Whitmarsh AJ, Yang DD et al (2003) A critical role of neural-specific JNK3 for ischemic apoptosis. Proc Natl Acad Sci USA 100:15184–15189

33. Kuan CY, Yang DD, Samanta Roy DR, Davis RJ, Rakic P, Flavell RA (1999) The Jnk1 and Jnk2 protein kinases are required for regional specific apoptosis during early brain development. Neuron 22:667–676

34. Ladd-Acosta C, Pevsner J, Sabunciyan S et al (2007) DNA methylation signatures within the human brain. Am J Hum Genet 81:1304–1315

35. Laffaire J, Everhard S, Idbaih A et al (2011) Methylation profiling identifies 2 groups of gliomas according to their tumorigenesis. Neuro Oncol 13:84–98

36. Liang P, Song F, Ghosh S et al (2011) Genome-wide survey reveals dynamic widespread tissue-specific changes in DNA methylation during development. BMC Genomics 12:231

37. Liu RZ, Mita R, Beaulieu M, Gao Z, Godbout R (2010) Fatty acid binding proteins in brain development and disease. Int J Dev Biol 54:1229–1239

38. Louis DN, Ohgaki H, Wiestler OD et al (2007) The 2007 WHO Classification of Tumours of the Central Nervous System. Acta Neuropathol (Berl) 114:97–109

39. Ma XJ, Salunga R, Tuggle JT et al (2003) Gene expression profiles of human breast cancer progression. Proc Natl Acad Sci USA 100:5974–5979

40. Mack SC, Taylor MD (2009) The genetic and epigenetic basis of ependymoma. Childs Nerv Syst 25:1195–1201

41. Mao R, Wang X, Spitznagel EL Jr et al (2005) Primary and secondary transcriptional effects in the developing human Down syndrome brain and heart. Genome Biol 6:R107

42. Martin JH, Mohit AA, Miller CA (1996) Developmental expression in the mouse nervous system of the p493F12 SAP kinase. Brain Res Mol Brain Res 35:47–57

43. Matallanas D, Romano D, Yee K et al (2007) RASSF1A elicits apoptosis through an MST2 pathway directing proapoptotic transcription by the p73 tumor suppressor protein. Mol Cell 27:962–975

44. McCabe MT, Brandes JC, Vertino PM (2009) Cancer DNA methylation: molecular mechanisms and clinical implications. Clin Cancer Res 15:3927–3937

45. McGuire CS, Sainani KL, Fisher PG (2009) Both location and age predict survival in ependymoma: a SEER study. Pediatr Blood Cancer 52:65–69

46. Michalowski MB, de Fraipont F, Michelland S et al (2006) Methylation of RASSF1A and TRAIL pathway-related genes is frequent in childhood intracranial ependymomas and benign choroid plexus papilloma. Cancer Genet Cytogenet 166:74–81

47. Miremadi A, Oestergaard MZ, Pharoah PD, Caldas C (2007) Cancer genetics of epigenetic genes. Hum Mol Genet 16 Spec No 1:R28–R49

48. Modena P, Lualdi E, Facchinetti F et al (2006) Identification of tumor-specific molecular signatures in intracranial ependymoma and association with clinical characteristics. J Clin Oncol 24: 5223–5233

49. Noushmehr H, Weisenberger DJ, Diefes K et al (2010) Identification of a CpG island methylator phenotype that defines a distinct subgroup of glioma. Cancer Cell 17:510–522

50. Oster B, Thorsen K, Lamy P et al (2011) Identification and validation of highly frequent CpG island hypermethylation in colorectal adenomas and carcinomas. Int J Cancer 129(12): 2855–2866

51. Owada Y, Yoshimoto T, Kondo H (1996) Spatio-temporally differential expression of genes for three members of fatty acid binding proteins in developing and mature rat brains. J Chem Neuroanat 12:113–122

52. Palm T, Figarella-Branger D, Chapon F et al (2009) Expression profiling of ependymomas unravels localization and tumor grade-specific tumorigenesis. Cancer 115:3955–3968

53. Pancione M, Di Blasi A, Sabatino L et al (2011) A novel case of rhabdoid colon carcinoma associated with a positive CpG island methylator phenotype and BRAF mutation. Hum Pathol 42(7): 1047–1052

54. Pfaffl MW (2001) A new mathematical model for relative quantification in real-time RT-PCR. Nucleic Acids Res 29:e45

55. Pike BL, Greiner TC, Wang X et al (2008) DNA methylation profiles in diffuse large B-cell lymphoma and their relationship to gene expression status. Leukemia 22:1035–1043

56. Rauch TA, Zhong X, Wu X et al (2008) High-resolution mapping of DNA hypermethylation and hypomethylation in lung cancer. Proc Natl Acad Sci U S A 105:252–257

57. Richter AM, Pfeifer GP, Dammann RH (2009) The RASSF proteins in cancer; from epigenetic silencing to functional characterization. Biochim Biophys Acta 1796:114–128

58. Rousseau E, Ruchoux MM, Scaravilli F et al (2003) CDKN2A, CDKN2B and p14ARF are frequently and differentially methylated in ependymal tumours. Neuropathol Appl Neurobiol 29: 574–583

59. Schwartzbaum JA, Huang K, Lawler S, Ding B, Yu J, Chiocca EA (2010) Allergy and inflammatory transcriptome is predominantly negatively correlated with CD133 expression in glioblastoma. Neuro Oncol 12:320–327

60. Smiraglia DJ, Rush LJ, Fruhwald MC et al (2001) Excessive CpG island hypermethylation in cancer cell lines versus primary human malignancies. Hum Mol Genet 10:1413–1419

61. Suzuki R, Shimodaira H (2006) Pvclust: an R package for assessing the uncertainty in hierarchical clustering. Bioinformatics 22:1540–1542

62. Taylor MD, Poppleton H, Fuller C et al (2005) Radial glia cells are candidate stem cells of ependymoma. Cancer Cell 8:323–335

63. Toyota M, Ahuja N, Ohe-Toyota M, Herman JG, Baylin SB, Issa JP (1999) CpG island methylator phenotype in colorectal cancer. Proc Natl Acad Sci U S A 96:8681–8686

64. Waha A, Koch A, Hartmann W et al (2004) Analysis of HIC-1 methylation and transcription in human ependymomas. Int J Cancer 110:542–549

65. Wang Q, Williamson M, Bott S et al (2007) Hypomethylation of WNT5A, CRIP1 and S100P in prostate cancer. Oncogene 26:6560–6565

66. Wei J, Barr J, Kong LY et al (2010) Glioma-associated cancer-initiating cells induce immunosuppression. Clin Cancer Res 16: 461–473

67. Weisenberger DJ, Siegmund KD, Campan M et al (2006) CpG island methylator phenotype underlies sporadic microsatellite instability and is tightly associated with BRAF mutation in colorectal cancer. Nat Genet 38:787–793

68. Wright KD, Gajjar A (2009) New chemotherapy strategies and biological agents in the treatment of childhood ependymoma. Childs Nerv Syst 25:1275–1282

69. Xie H, Wang M, Bonaldo Mde F et al (2010) Epigenomic analysis of Alu repeats in human ependymomas. Proc Natl Acad Sci U S A 107:6952–6957

70. Xu PX, Adams J, Peters H, Brown MC, Heaney S, Maas R (1999) Eya1-deficient mice lack ears and kidneys and show abnormal apoptosis of organ primordia. Nat Genet 23:113–117

71. Yang DD, Kuan CY, Whitmarsh AJ et al (1997) Absence of excitotoxicity-induced apoptosis in the hippocampus of mice lacking the Jnk3 gene. Nature 389:865–870

72. Ying J, Li H, Cui Y, Wong AH, Langford C, Tao Q (2006) Epigenetic disruption of two proapoptotic genes MAPK10/JNK3 and PTPN13/FAP-1 in multiple lymphomas and carcinomas through hypermethylation of a common bidirectional promoter. Leukemia 20:1173–1175

73. Yoshida S, Fukino K, Harada H et al (2001) The c-Jun NH2-terminal kinase3 (JNK3) gene: genomic structure, chromosomal assignment, and loss of expression in brain tumors. J Hum Genet 46:182–187

74. Yuen RK, Neumann SM, Fok AK et al (2011) Extensive epigenetic reprogramming in human somatic tissues between fetus and adult. Epigenetics Chromatin 4:7

75. Zacharoulis S, Levy A, Chi SN et al (2007) Outcome for young children newly diagnosed with ependymoma, treated with intensive induction chemotherapy followed by myeloablative chemotherapy and autologous stem cell rescue. Pediatr Blood Cancer 49:34–40

76. Zou H, Osborn NK, Harrington JJ et al (2005) Frequent methylation of eyes absent 4 gene in Barrett's esophagus and esophageal adenocarcinoma. Cancer Epidemiol Biomarkers Prev 14:830–834